https://doi.org/10.1016/j.diamond.2021.108290

Combined electrical resistivity-electron reflectivity measurements for evaluating the homogeneity of hydrogen-terminated diamond surfaces

V.Serpente[1,2,*], A. Bellucci[1], M. Girolami[1], M. Mastellone[1], S. Iacobucci[1,2], A. Ruocco[2], and D.M. Trucchi[1]

[1]*Istituto di Struttura della Materia ISM-CNR, DiaTHEMA Lab, Via Salaria km 29.300, 00015 Monterotondo, Rome, Italy*
[2]*Dipartimento di Scienze, Università degli Studi Roma Tre, Via della Vasca Navale 84, 00146 Rome, Italy*

Abstract: The homogeneity of hydrogen termination on single-crystal CVD diamond surfaces exposed to air was studied with a new approach that encloses a combination of sheet resistance measurements, performed using four-point-probe method in Van Der Pauw configuration, and electron reflectivity measurements performed at intermediate kinetic energy to derive surface sensitive information on the chemical terminations (inelastic mean free path <0.8 nm). The coherence between the 2-dimensional spatial distributions of sheet resistance and electron reflectivity maps, as well as their similar dynamic range and consistency with an electron energy loss analysis, demonstrates that the proposed combined approach allows for a reliable and easy evaluation of both the effectiveness and homogeneity of the hydrogen-termination process of a diamond surface.

Keywords: Hydrogenated diamond; Surface conductivity; Resistivity mapping; Electron reflectivity mapping; Electron Energy Loss Spectroscopy.

1. Introduction

Diamond is a well-known wide bandgap semiconductor [1], used mainly for ionising radiation [2-4], nuclear particles detectors [5] and, recently, in thermionic converters for concentrated solar energy [6]. Among diamond unique physical properties, such as the highest thermal conductivity observed amidst solids or the outstanding hardness [7], the surface p-type conductivity, originated by charge-transfer doping mechanism [8], has been exploited in the last decade for the fabrication of high-power high-frequency field-effect transistor (FET) prototypes [9, 10] with remarkable performance. Electrical conductivity is activated by terminating the diamond surface with hydrogen, and then simply exposing it to air; however, despite the mechanism of charge transport is already known, there are still open questions on the reproducibility of the process, as well as on the airborne species responsible for conductivity activation, hampering in this way the increase of the reliability of diamond-based electronic devices. In particular, there is lack of accurate information on the state of diamond surface when the conduction mechanism is activated, especially in terms of homogeneity in the hydrogen termination: earlier attempts to study hydrogenated diamond surfaces were indeed focused on the investigation of surface properties [11] or to better understand surface composition [12] and reconstruction [13]. Infrared spectroscopy (FTIR) has been employed to locally evaluate both hydrogen density and orientation [14, 15] while study on homogeneity were performed mainly by Raman spectroscopy analysis, for investigating the effects of stress and defects [16] in the bulk, therefore giving poor information about the surface.

In such a context, we introduce here an innovative approach based on the combination of two different methods: 1) sheet resistance measurements for locally monitoring the presence of macroscopic (electrical) effects and 2) spectroscopic measurements, performed by measuring the electron reflectivity and applying Electron Energy Loss Spectroscopy (EELS), for analysing the formation of microscopic (electronic and chemical) effects. Results shown in the following point out the effectiveness of using this combined approach in providing information on the homogeneity of a hydrogenated diamond surface, highlighting as well the potentiality of electron reflectivity measurements as a powerful tool for hydrogenated-diamond surface characterization, alternative to the already existent techniques.

2. Experimental

For this study, commercially available single-crystal 4.5×4.5×0.5 mm^3 (100) diamond plates (produced by Element Six Ltd) are used, characterized by a minimal presence of impurities (N and B atomic concentration are < 5 ppb and < 1 ppb, respectively). The hydrogenation of the samples is performed in a dedicated chamber, exposing them for one hour (heated at 700 °C) to a hydrogen microwave plasma (1.23 kW power, 2.45 GHz frequency), at a pressure of 40 mbar, similarly to the recipe used in [17]. After hydrogenation, the samples are exposed to air for some days: this allows the airborne species responsible for conductivity activation to have enough time to adsorb on the hydrogen-terminated surface.

Electric measurements are performed *in-situ* with a two-point probe method under high vacuum and temperature conditions, and *ex-situ* with a four-point probe method in the Van der Pauw configuration, covering a sampling area of 1×1 mm^2 and moved by a 2-axes micrometre translational stage, in air. A calibration in temperature was previously performed for the two-probe measurements in order to take into account the parasitic effect of the contact resistance. Furthermore, in order to consider the displacement of the four probes with respect to the centre of the sampling area, a correction factor is applied according to the calculation proposed by D.S. Perloff [18].

Electron reflectivity measurements and EELS are performed in an ultra-high vacuum chamber (base pressure

* Corresponding author. E-mail: valerio.serpente@ism.cnr.it

of 10^{-10} mbar) by using a 100 eV energy electron beam, with a total current of 70 pA delivered on a circular spot of 1 mm diameter (more details of the employed electron source can be found in Ref. 17). The used kinematics probe few topmost surface layers (the corresponding electron mean free path is estimated to be <0.8 nm [20, 21].

3. Results and Discussion

Once the sample is hydrogenated and air exposed, its sheet resistance is constantly monitored as a function of time, temperature and pressure during four stages, as evidenced in Fig. 1, which displays the sheet-resistance and the temperature as a function of time thus permitting to correlate the first two in between them: 1) initial evacuation process from atmospheric pressure down to a vacuum level of 10^{-6} mbar; 2) heating in vacuum from room temperature (RT) to T = 600 °C, 3) subsequent cooling down to RT in vacuum; 4) air exposure at RT. As can be inferred from Fig. 1, the sheet resistance increases by about two orders of magnitude (from about 3×10^4 to 10^6 Ω/sq.) during pressure reduction at RT. This can be explained by considering the increased desorption rate of airborne species from the hydrogenated surface, which causes a decrease of available charge carriers and, as a consequence, of electrical conductivity. When the base pressure of the chamber is reached (end of stage 1), a new balance condition is established between absorption and desorption rate of the active species present as residual gases in the chamber, and the sheet resistance reaches a new equilibrium value.

Within the heating stage, it is possible to distinguish from Fig. 1 two different behaviours, as highlighted in the corresponding insert that shows the sheet resistance as a function of temperature. Firstly, from 25 °C to about to about 500 °C, the sheet resistance increases with temperature of about 3 orders of magnitude (from 10^6 to 10^9 Ω/sq.): this behaviour is compatible with a progressive heat-activated desorption of atmospheric molecules, and a consequent decrease of surface charge carriers. Then, when T > 500 °C, the sheet resistance decreases slightly with temperature, falling again below 10^9 Ω/sq: this is most probably due to the temperature-driven activation of bulk semiconductor conductivity, which overcompensates for the decrease of surface charge carriers. As soon as vacuum cooling starts, bulk conductivity is rapidly quenched, and the sheet resistance starts increasing again due to active species desorption, until a new equilibrium condition (at about 10^{12} Ω/sq.) is reached at RT at pressure of 10^{-6} mbar. It's reasonable to assume that this condition corresponds to a complete desorption of all the adsorbates.

Finally, the sample is exposed *in-situ* again to air (stage 4). Note that the sheet resistance decreases of more than seven orders of magnitude (from 10^{12} Ω/sq. to 10^5 Ω/sq.) in only 30 minutes, before returning to the exact initial value (about 3×10^4 Ω/sq.) after approximately 14 hours since the beginning of the measurements. These results, as expected, highlight a complete recovery of electrical conductivity, as well as a transition from a non-conductive (simply H-terminated) to a conductive (H-terminated with adsorbates) diamond film. The significative difference in the measured sheet resistance values, larger than that observed by Maier [8], is probably related to the lower defect density (and higher amount of C-H bindings) of the electronic-grade samples used in this work.

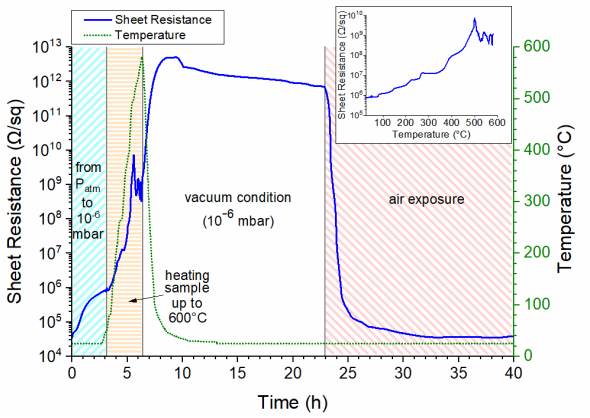

FIG. 1. Typical sheet resistance of the surface hydrogenated-diamond films as a function of time, temperature and pressure. The four measurement stages (see text) are also indicated. The inset of the figure highlights the behaviour of sheet resistance as a function of temperature.

Once performed the described electrical measurements, the hydrogen termination homogeneity of the sample surface is investigated *ex-situ* by mapping the sheet resistance in air and at RT. The resulting sheet resistance map is shown in Fig. 2. As it can be seen from the 2D map (Fig. 2a), as well as from the 1D spatial distribution recorded from a central section (Fig. 2b), the left half of the sample surface shows a fairly homogeneous sheet resistance in the range 14 – 16 kΩ/sq (that, taking in account a hole mobility in air and at RT of about 100 cm^2/Vs, corresponds to a hole sheet density of about 4×10^{12} cm^{-2}, in agreement with previous literature [22]), whereas the right half is dominated by a small spot with an almost doubled sheet resistance (up to 25 kΩ/sq) than the left half. Therefore, it is reasonable to suppose that different zones of the sample surface are chemically-terminated in different ways (or have different density of physisorbed adsorbates).

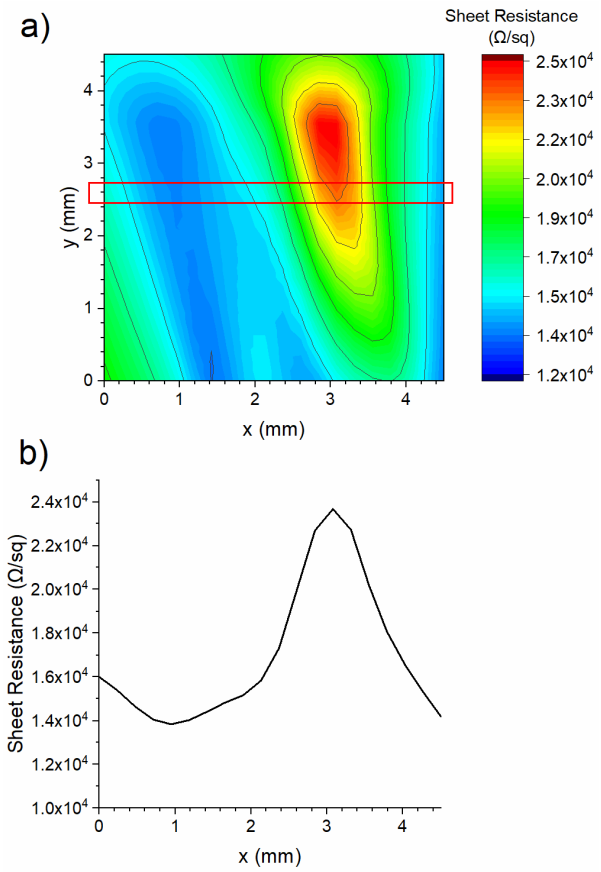

FIG. 2. a) Sheet resistance map obtained for the sample hydrogenated surface, corrected according to the Perloff's method [18]; b) 1D spatial distribution of the sheet resistance along x-axis (measured at a fixed y value, as highlighted by the red box in Fig. 2a).

A simple way to validate this hypothesis is probing the sample surface with an electron beam of sufficiently low energy, recording the elastically backscattered electrons in specular configuration, i.e. with (angle-resolved) electron reflectivity measurements. The idea behind is to exploit the surface sensitivity of low energy electrons to gather local information on the structure of the surface for the sample under investigation. The reflectivity is mapped along the whole hydrogen-terminated diamond surface: results are shown in Fig. 3.

It can be clearly noticed in Fig.3a the similarity with the sheet resistance map of Fig. 2a, implying that there is a strong correlation between the number of reflected electrons and the value of the sheet resistance. It is also worth noting in Fig. 3b that the dynamic range of the reflected electron counts (varying from 15×10^3 to 28×10^3 counts/s) in the same central zone considered in Fig. 2b, is very similar to the dynamic range of sheet resistance (varying in the same zone from 14 to 25 kΩ/sq.). So, we can deduce that: 1) the higher the electron reflectivity, the higher the sheet resistance measured; 2) the increase of electron reflectivity is approximately of the same amount of the increase of sheet resistance. These observations suggest that diamond surface zones covered with hydrogen and electrically activated by the presence of adsorbates are probably less ordered (thus spreading the electrons in angle with a reduction of the intensity recorded in specular direction) comparing to zones characterized by the absence of adsorbates (i.e. in the case of bare surface).

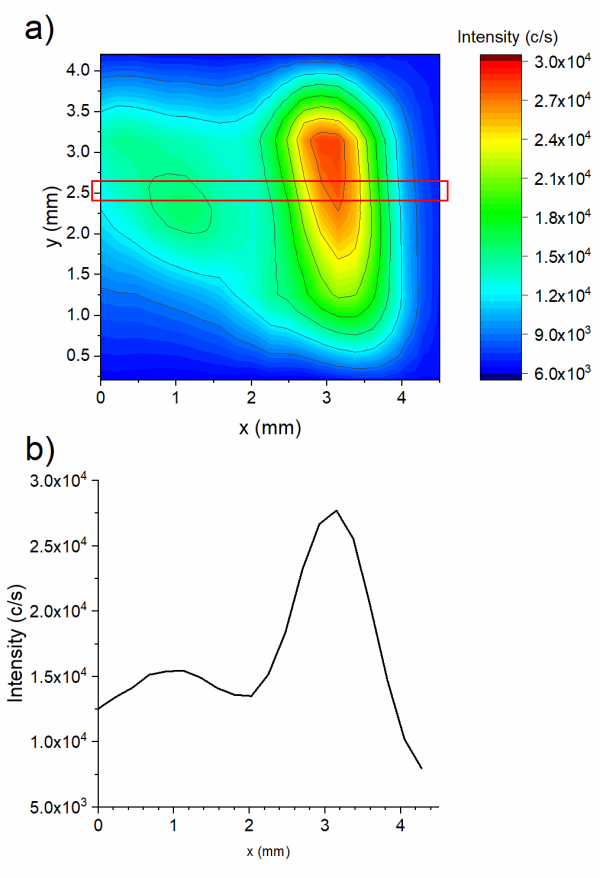

FIG. 3. a) Electron reflectivity map of the sample surface obtained by counting elastically backscattered electrons; b) 1D spatial distribution of the electron reflectivity along x-axis (measured at a fixed y value, as highlighted by the red box in Fig. 3a). The fixed y value (y = 2.5mm) is the same as the one chosen for the sheet resistance 1D spatial distribution reported in Fig. 2a.

In this context, EELS is a powerful surface-sensitive technique able to further shed a light on the different behaviors observed in both the sheet resistance and electron reflectivity maps.

Fig. 4 reports EELS measurements performed in two selected zones: low resistivity-low reflectivity (LRR, black curve) and high resistivity-high reflectivity (HRR,

red curve). The two spectra are very similar in the 10 – 50 eV energy loss region, where the typical features of diamond are present: a feature located at 14 eV, related to transition from valence to conduction band [23], and two features at 23 and 33 eV due to surface and bulk plasmons [13, 24-26], respectively. Conversely, the main differences are located in the low energy loss region 2 – 10 eV, which represents a benchmark for the surface termination of diamond [24]. In particular, note that the signal recorded from the LRR zone is significantly less intense than that recorded from the HRR zone in the same energy loss range and that the LRR curve is steeper. By comparing the spectra of Fig. 4 to those reported in Ref. 16 on hydrogenated, oxidized and bare diamond surfaces, it is possible to infer that HRR spectrum (showing a smoother slope in the 5 – 10 eV range) is more similar to that obtained from a bare diamond surface, whereas LRR spectrum is a fingerprint of densely-hydrogenated surfaces. This is reasonable, being hydrogenation a necessary requirement for diamond p-type surface conductivity.

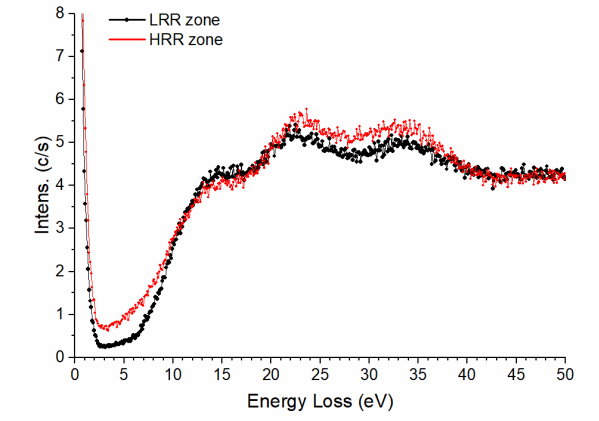

FIG. 4. Electron energy loss spectra record from low resistivity-low reflectivity (LRR) and high resistivity-high reflectivity (HRR) zones of the sample. Experimental setup was the same as the one used for electron reflectivity measurements. Electron beam energy was 100 eV, whereas pass energy was set to 2 eV.

It is also worth spending a few words on the possible explanation of the non-uniform hydrogenation of samples. Most probably, they might not be symmetrically placed under the hydrogen plasma; if it occurs, the zones of the surface closest to the hydrogen plasma have more chance to be more effectively and densely hydrogenated than the farthest ones. Also, non-homogeneity can be related to the pinning of the hydrogen plasma to one point of the diamond surface, causing an excessive increase of local temperature, and therefore altering the optimal conditions for hydrogen sticking.

4. Conclusions

By comparing the electrical resistivity (sheet resistance) with electron scattering experiments on a hydrogenated-diamond surface we have put in evidence the direct correlation between the 2D resistance pattern with spatial distributions of both elastically and inelastically reflected electrons. We have found that low resistivity zones are also characterized by low electron reflectivity. EELS measurements further point out that low resistivity-low reflectivity zones are more densely hydrogenated than high resistivity-high reflectivity ones. Our findings result in a powerful approach to characterize effectiveness and homogeneity of the hydrogen-termination process.

We suppose that non-homogeneity effects may arise from a non-symmetrical placement under the plasma or from local increasing of temperature, issues that can affect the reliability and reproducibility of the hydrogenation process for the surface p-type conductivity of a diamond film, the homogeneity of which can be anyway easily and accurately verified with the combined approach we propose in this work.

References

[1] R. Sussmann, CVD Diamond for Electronic Devices and Sensors, Chichester, UK: John Wiley & Sons, 2009.

[2] M. Girolami, A. Bellucci, P. Calvani, R. Flammini and D. M. Trucchi, *Appl. Phys. Lett.,* 103, 083502 (2013), doi: 10.1063/1.4818904.

[3] D.M. Trucchi, P. Allegrini, A. Bellucci, P. Calvani, A. Galbiati, M. Girolami, Nucl. Instrum. Methods Phys. Res., Sect. A 718, 373-375 (2013), doi: 10.1016/j.nima.2012.10.095.

[4] M. Girolami, A. Bellucci, P. Calvani, and D.M. Trucchi, Phys. Status Solidi A 213, 2634-2640 (2016), doi: 10.1002/pssa.201600262.

[5] A. Muraro, L. Giacomelli, M. Nocente, M. Rebai, D. Rigamonti, F. Belli, P. Calvani, J. Figueiredo, M. Girolami, G. Gorini, G. Grosso, A. Murari, S. Popovichev, D. M. Trucchi, M. Tardocchi, and JET Contributors, Rev. Sci. Instrum. 87, 11D833 (2016), doi: 10.1063/1.4961557.

[6] D.M. Trucchi, A. Bellucci, M. Girolami, P. Calvani, E. Cappelli, S. Orlando, R. Polini, L. Silvestroni, D. Sciti, A. Kribus, Adv. Energy Mater. 8, 1802310 (2018), doi: 10.1002/aenm.201802310.

[7] C. Wort, Materials Today 11, 22 (2008), doi: 10.1016/S1369-7021(07)70349-8.

[8] F. Maier, D. Riedel, B. Mantel, J. Ristein, L. Ley, Phys. Rev. Lett. 85, 3472 (2000), doi: 10.1103/PhysRevLett.85.3472.

[9] P. Calvani, A. Corsaro, M. Girolami, F. Sinisi, D.M. Trucchi, M.C. Rossi, G. Conte, S. Carta, E. Giovine, S. Lavanga, E. Limiti, V. Ralchenko, Diam. Relat. Mater. 18, 786 (2009), doi: 10.1016/j.diamond.2009.01.014.

[10] K. Ueda, M. Kasu, Y. Yamauchi, T. Makimoto, M. Schwitters, D.J. Twitchen, G.A. Scarsbrook, S.E. Coe, IEEE

Electron Device Lett., 27, 570-572 (2016), doi: 10.1109/led.2006.876325.
[11] J. Shirafuji, T. Sugino,, Dia. Relat. Mater. 5, 706-713 (1996), doi: 10.1016/0925-9635(95)00415-7
[12] R. Graupner, F. Maier, J. Ristein, L. Ley, C. Jung, Phys. Rev. B 57, 12397-12409 (2000), doi: 10.1103/PhysRevB.57.12397.
[13] P.E. Pehrsson and T.W. Mercer, Surf. Sci. 460, 49 (2000), doi: 10.1016/S0039-6028(00)00495-7.
[14] R. P. Chin, Y. Huang, R. Shen, T. J. Chuang, H. Seki and M. Buck, Phys. Rev. B. 45, 1522-1524 (1992), doi: 10.1103/PhysRevB.45.1522.
[15] R. P. Chin, J. Y. Huang, Y. R. Shen, T. J. Chuang, and H. Seki, Phys. Rev. B 52, 5985-5995 (1995), doi: 10.1103/PhysRevB.52.5985.
[16] A. Haouni, M. Mermoux, B. Marcus, L. Abello, G. Lucazeau, Dia. Relat Mater. 8, 657-662 (1999), doi: 10.1016/S0925-9635(98)00253-2.
[17] S. Iacobucci, P. Alippi, P. Calvani, M. Girolami, F. Offi, L. Petaccia, D. M. Trucchi, Phys. Rev. B 94, 045307 (2016), doi: 10.1103/PhysRevB.94.045307.
[18] D.S. Perfloff, Solid-State Electron. 20, 681 (1977), doi: 10.1016/0038-1101(77)90044-2.
[19] G.M. Pierantozzi, M. Sbroscia, A. Ruocco, Surf. Sci. 669, 176-182 (2018), doi: 10.1016/j.susc.2017.12.003.
[20] M.P. Seah, W.A. Dench, Surf. Interface Anal. 1, 2-11 (1979), doi: 10.1002/sia.740010103.
[21] B. Ziaja, R. A. London, J. Hajdu, J. App. Phys. 99, 033514 (2006), doi: 10.1063/1.2161821
[22] Y. Wang, H. Chen and R. Hoffman, J. Mater. Res. 5, 2378 (1990), doi: 10.1557/jmr.1990.2378.
[23] B. Rezek, H. Watanabe, and C. E. Nebel, Appl. Phys. Lett. 88, 042110 (2006), doi: 10.1063/1.2168497.
[24] E.A. Maydell et al., Diam. Relat. Mater. 2, 873 (1993), doi: 10.1016/0925-9635(93)90242-T.
[25] P. E. Pehrsson and T. W. Mercer, Surf. Sci. 497, 13 (2002), doi: 10.1016/S0039-6028(01)01677-6.
[26] Y. Fan et al., Surf. Interface Anal. 34, 703 (2002), doi: 10.1002/sia.1392.